Submitted to ApJL. Manuscript LET00000
Preprint typeset using LaTeX style emulateapj v. 5/2/11

ROTATION PERIODS AND AGES OF SOLAR ANALOGS AND SOLAR TWINS REVEALED BY THE *KEPLER* MISSION

J.-D. do Nascimento, Jr.[1,2], R. A. García[3], S. Mathur[4], F. Anthony[2], S. A. Barnes[5], S. Meibom[1], J.S. da Costa[2], M. Castro[2], D. Salabert[3] and T. Ceillier[3]

Submitted to ApJL. Manuscript LET00000

ABSTRACT

A new sample of solar analogs and twin candidates have been constructed and studied, with particular attention to their light curves from NASA's *Kepler* mission. This letter aims to assess the evolutionary status, derive their rotation and ages and identify those solar analogs or solar twin candidates. We separate out the subgiants that compose a large fraction of the asteroseismic sample, and which show an increase in the average rotation period as the stars ascend the subgiant branch. The rotation periods of the dwarfs, ranging from 6 to 30 days, and averaged 19d, allow us to assess their individual evolutionary states on the main sequence, and to derive their ages using gyrochronology. These ages are found to be in agreement with a correlation coefficient of r = 0.79 with the independent asteroseismic ages, where available. As a result of this investigation, we are able to identify 34 stars as solar analogs and 22 of them as solar twin candidates.

Subject headings: stars: evolution — stars: fundamental parameters stars, — stars: rotation, — stars: solar-type, — Sun: fundamental parameters

1. INTRODUCTION

The Sun is a benchmark in stellar astrophysics research and establishing a sample of solar analog stars is important to map its past, present and future. About 50 yr ago, Olin Wilson and collaborators discovered Sun-like activity cycles in a group of ~ 100 stars, now known as the Mt. Wilson sample (Wilson 1963). Additional work over the intervening decades (e.g., Noyes *et al.* 1984) has made us confident that some of these stars do indeed have ages comparable to that of the Sun and that their activity, and chemical and other fundamental properties make them, in many ways, "solar analogs". Many additional studies have allowed the identification of some other stars as solar analogs and some of these have properties that are close enough to those of the Sun that they are even called "solar twins". Solar twins are spectroscopically indistinguishable from the Sun (Cayrel de Strobel 1996) for example, 18 Sco (Porto de Mello & da Silva 1997; Bazot *et al.* 2011), CoRoT Sol 1 (do Nascimento *et al.* 2013), and HIP 102152 (Monroe *et al.* 2013). The term "solar analogs" here refers to stars with $0.9 < M/M_{\odot} \leq 1.1$ and "solar twin candidates" refers to stars with $0.95 < M/M_{\odot} \leq 1.05$ and rotation periods of $P_{\rm rot} > 14$ days.

Solar twins also allow us to decide to what extent the Sun itself can be considered a "typical" 1.0 $M_{\odot}$ star (Gustafsson 2008). The search for solar twins has been greatly expanded since 1997 (Hardorp 1978; Cayrel de Strobel 1996), when only one solar twin was known, and currently more than two dozen twins have been identified (e.g., Meléndez & Ramírez 2007; do Nascimento *et al.* 2013; Monroe *et al.* 2013). Solar twins are also important to calibrate fundamental UBV(RI)$_C$ — $T_{\rm eff}$ relations (Porto de Mello & da Silva 1997; Ramírez *et al.* 2012) and to test non-standard stellar models (e.g., Bazot *et al.* 2011). A sample of solar twins with determined $P_{\rm rot}$ is also important to study the "Sun in Time" (see Dorren & Guinan 1994).

A related consideration is how the Sun has changed over time, and how its behavior relates to that of other younger and older stars of solar mass. Studying this requires that we assemble a sample of stars whose ages we know well enough to place them all in a time sequence that includes the Sun. However, ages for field stars, particularly for those on the main sequence, are notoriously difficult to derive (e.g., Barnes 2007; Soderblom 2010). Consequently, the classical distinction between solar-type and analogs or twins does not include age constraints apart from the obvious dwarf/giant distinction. The various requirements make finding solar analogs and twins difficult. A good way to find such valuable stars is to take advantage of space missions such as *CoRoT* (Baglin *et al.* 2006) and NASA's *Kepler* mission (Borucki *et al.* 2010). These missions have provided precise observations for thousands of main-sequence stars. Furthermore, we can detect periodic stellar variability for these stars. Such modulation is a signature of the presence of spots on the star's surface and can be used to measure the stellar $P_{\rm rot}$ (e.g., Basri *et al.* 2011; Meibom *et al.* 2011; do Nascimento *et al.* 2013; McQuillan *et al.* 2013). From $P_{\rm rot}$, ages can be estimated using gyrochronology (Barnes 2007).

Although recent works have increased the number of solar twins and studied their physical parameters and chemical abundances in detail, their $P_{\rm rot}$ are mostly unknown, except for the two solar twins 18 Sco (Porto de Mello & da Silva 1997) and CoRoT Sol 1

[1] Harvard-Smithsonian Center for Astrophysics, Cambridge, MA 02138, USA; jdonascimento@cfa.harvard.edu
[2] Universidade Federal do Rio Grande do Norte, UFRN, Dep. de Física Teórica e Experimental, DFTE, CP 1641, 59072-970, Natal, RN, Brazil
[3] Laboratoire AIM, CEA/DSM – CNRS -, Univ. Paris Diderot – IRFU/SAp, Centre de Saclay, F-91191 Gif-sur-Yvette Cedex, France
[4] Space Science Institute, 4750 Walnut Street Suite 205, Boulder CO 80301, USA
[5] Leibniz-Institute for Astrophysics, Potsdam D-14467, Germany

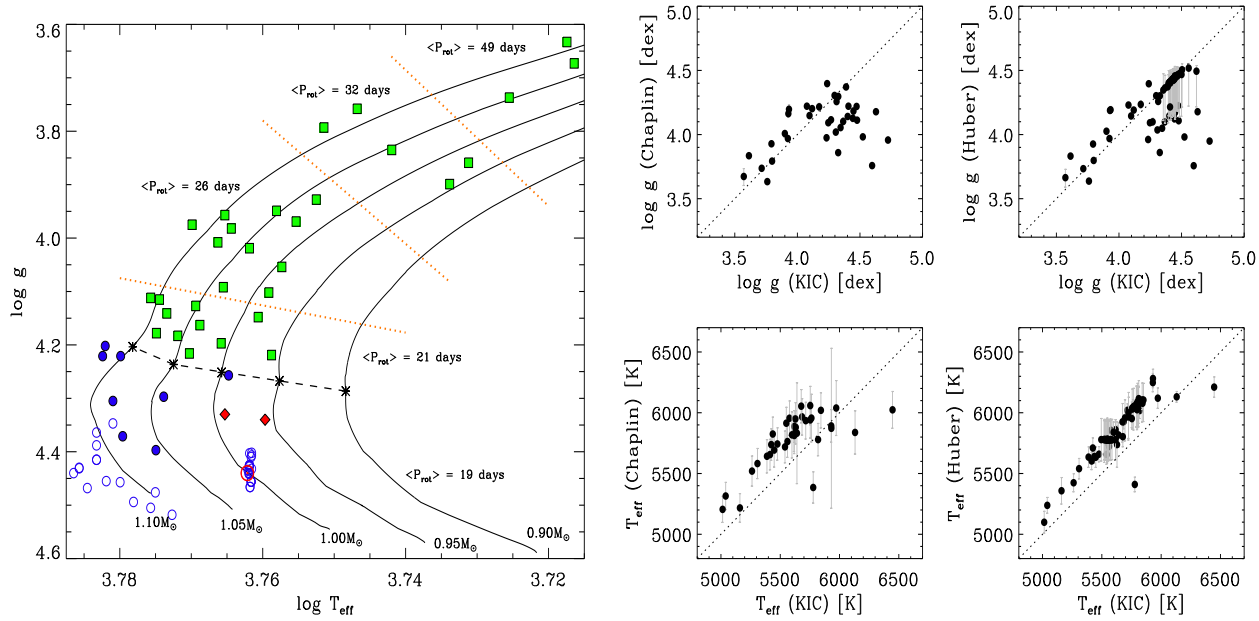

Figure 1. Large panel on the left shows the $\log g$ - $T_{\rm eff}$ for the entire sample. Open circles represent dwarfs selected from the KIC and filled circles dwarfs from the seismic sample. Squares represent subgiants. Diamonds indicate 16 Cyg A and B evolutionary status. The upper panels on the right compare the $\log g$ values of Chaplin *et al.* (2014) and Huber *et al.* (2014) to the KIC values. The bottom panels of the right compare the corresponding $T_{\rm eff}$ values.

(do Nascimento *et al.* 2013).

2. WORKING SAMPLE

Our sample of 75 stars consists of a *seismic sample* of 38 from Chaplin *et al.* (2014), 35 additional stars selected from the *Kepler* Input Catalog (KIC), and 16 Cyg A and B. We selected 38 well-studied stars from the asteroseismic data with fundamental properties, including ages, estimated by Chaplin *et al.* (2014), and with $T_{\rm eff}$ and $\log g$ as close as possible to the Sun's value (5200 K $< T_{\rm eff} <$ 6060 K and $3.63 < \log g < 4.40$). This seismic sample allows a direct comparison between gyro and seismic–ages for a subset of eight stars. These *seismic sample* were observed in short cadence for one month each in survey mode. Stellar properties for these stars have been estimated using two global asteroseismic parameters and complementary photometric and spectroscopic observations as described by Chaplin *et al.* (2014). The median final quoted uncertainties for the full Chaplin *et al.* (2014) sample were approximately 0.020 dex in $\log g$ and 150 K in $T_{\rm eff}$.

The 35 selected stars from the improved version of the KIC (Brown *et al.* 2011, Huber *et al.* 2014) present stellar parameters $T_{\rm eff}$ and $\log g$ in the range 5700 K $\leq T_{\rm eff} \leq$ 6120 K and $4.3 \leq \log g \leq 4.6$. The median final quoted uncertainties were approximately [+0.070, -0.280] dex in $\log g$ and 160 K in $T_{\rm eff}$. We derived isochrone ages for these stars. We also included the well–studied solar analogs 16 Cyg A and B (KIC 12069424 and 12069449; V∼6), with estimated ages of $t = 6.8 \pm 0.4$ Gyr for both stars. (Metcalfe *et al.* 2012; Lund *et al.* 2014). So far, for 16 Cyg A & B, there have been no direct measurements of surface rotation. The age implies that $P_{\rm rot}$ should be near 30 days (Skumanich 1972, Barnes 2010) for both components. Table 1 summarizes the properties of our targets. The sample is displayed in Figure 1.

3. EVOLUTIONARY STATUS

We used models computed with the Toulouse-Geneva stellar evolution code (Hui-Bon-Hoa 2008, Richard *et al.* 1996; do Nascimento *et al.* 2013). These models used an initial composition with the Grevesse & Noels (1993) mixture. Rotation-induced mixing and the transport of angular momentum due to rotationally induced instabilities are computed as described by Talon & Zahn (1997), and these models take into account internal differential rotation. The angular momentum evolution follows the Kawaler (1988) prescription. Our solar model is calibrated to match the observed solar $T_{\rm eff}$, luminosity, and rotation at solar age (Richard *et al.* 1996). Models are shown in Figure 1 (left). We have computed standard (without rotation) and non-standard models for stellar masses between 0.9 and 1.1 $M_{\odot}$ and for different metallicities consistent with the range of our sample stars. To discriminate between dwarfs and subgiants, models are shown with a dashed black line that indicates the evolutionary point where the subgiant branch starts and which corresponds to hydrogen exhaustion in the stellar core (i.e., turnoff point). The 30 stars above this line are subgiants. The remaining 45 stars below this line are dwarfs and of primary interest here. From these, eight are dwarfs with ages known from asteroseismology. Finally, we determine the individual masses of our sample of dwarf stars by using the evolutionary tracks for the respective metallicities. From this, most of the mass determination uncertainty is due to the uncertainties on $T_{\rm eff}$ (∼150K) which lead to an error of ∼0.05 $M_{\odot}$. Our determined values agree with those of Huber *et al.* (2014). For dwarfs, the mass determination is negligibly affected by the choice of standard or non-standard models, and the uncertainties are smaller than intrinsic errors in the $\log g$ and $T_{\rm eff}$. The mass determination uncertainties become significant for subgiants.

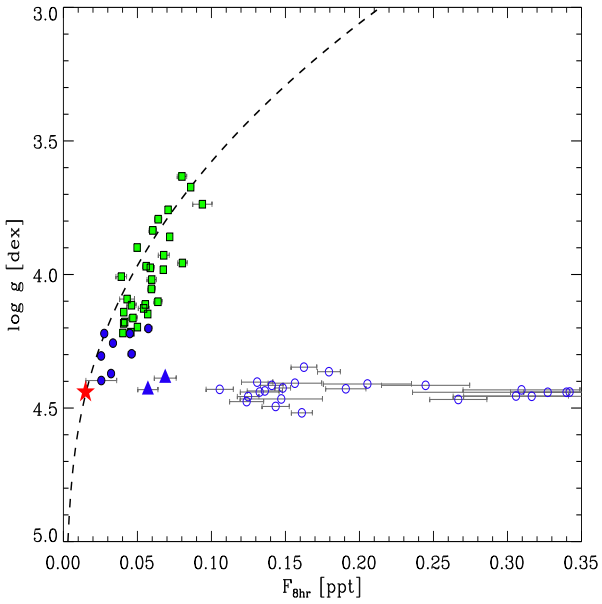

Figure 2. Surface gravity from asteroseismology (filled squares and circles) determined by Chaplin *et al.* 2014 and from the Huber *et al.* (2014) (open circles) as a function of the 8-hour flicker F_8, (Bastien *et al.* 2013). Circles represent dwarfs and squares represent the subgiants. The black dashed line corresponds to the relationship derived by Bastien *et al.* (2013). The red symbol at lower left represents the Sun $\log g$ and F_8. Filled triangle represent KIC 2718678, and KIC 12157617.

4. EXTRACTING THE SURFACE ROTATION RATES

The average surface $P_{\rm rot}$ is obtained from light curve modulation analysis. To extract the $P_{\rm rot}$, we analyze PDC-MAP and simple aperture photometry light curves (Christiansen *et al.* 2013) that are corrected for outliers, drifts, and discontinuities and stitched together following the procedures described by García *et al.* (2011). The light curves are then high-pass filtered using a triangular smooth function with a cut-off that can change from 40 to 100 days. We remind readers that the PDC-msMAP (Christiansen *et al.* 2013) corrected data proposed by *Kepler* cannot be used here, because some quarters are filtered with a 20 day high-pass filter (García *et al.* 2014). From a Lomb–Scargle periodogram (Scargle 1982), we searched for the highest peaks below 11.57 μHz with one daily alias. To ensure that the retrieved peaks are due to stellar signals, we verified that the signal responsible for the $P_{\rm rot}$ is present during most of the observed window. Then, we visually examined the results and any period detected was considered robust if repeated features were visible in different parts of the light curve. Finally, we computed the autocorrelation of the signal (McQuillan *et al.* 2013) in order to cross-check the results. We fit a Gaussian function to the global wavelet spectrum (Mathur *et al.* 2010), i.e., the projection into the frequency domain of the time frequency analysis and the uncertainty was obtained from the full width at half-maximum of the Gaussian profile. This uncertainty includes the $P_{\rm rot}$ variation due to differential rotation. Our entire sample is composed of 75 stars, and their derived periods and errors are presented in Table 1.

5. KIC PARAMETERS AND FLICKER MEASURES

In order to better interpret $P_{\rm rot}$, it is important to get an idea of how reliable the fundamental parameters (Silva Aguirre *et al.* 2012) are. We compared the KIC parameters with those determined by Chaplin *et al.* (2014) and with revised Huber *et al.* (2014) values for all of the stars of the seismic sample and solar analogs and twin candidates, see Figure 1 (right). The $T_{\rm eff}$ from the KIC is systematically lower when compared to values based on the asteroseismic analysis (Figure 1, bottom right panel). Huber *et al.* (2014) incorporated priors results in the distributions of the parameters at fixed temperature and used colors (e.g., $J-K$, $H-K$, $g-i$) with little sensitivity to [Fe/H] to arrive at more realistic distributions around 0.01 dex in $\log g$. We adopted the Huber *et al.* (2014) values.

We have measured the "flicker" as defined by Bastien *et al.* (2013) and validated by Cranmer *et al.* (2014), as a proxy of the granulation properties that scale with the stellar $\log g$ (Mathur *et al.* 2011). Since we analyzed 1440 days of data, we slightly modify the method by dividing the time series into *Kepler* quarters (where Q1 is a month long and the following quarters are each three months) and we computed the standard deviation of each sub-series smoothed over an eight hour boxcar (the same results were obtained using a six hour function). We then corrected the values for the photon noise (Jenkins *et al.* 2011). We applied this procedure to our entire sample. In Figure 2, we display $\log g$ as a function of the eight hour flicker F_{8hr} which we measured. For the filled symbols (dwarfs and subgiants), we can clearly see the correlation as shown by Bastien *et al.* (2013). The red star represents the Sun's $\log g$, fixed at $\log g = 4.44$, and flicker F_{8hr} (Bastien *et al.* 2013). We can distinguish two stars (filled triangle), namely KIC 2718678 ($V \sim 11.49$) and KIC 12157617 ($V \sim 11.89$), located close to the position of the Sun. Based on Bastien *et al.* (2013), this plot suggests that these two stars are more likely to be very similar to the Sun from their activity level, as measured by the eight hour flicker F_{8hr}. A second group of stars has similar values of $\log g$ and with a wide range of flicker F_{8hr}. These stars are represented by open circles belonging to the large-flicker horizontal line shift away from the dashed line. Those might be stars with an activity level at the mid-point of their cycle that is larger than the Sun's at solar maximum. They might be stars younger than the Sun or stars expected to have a higher noise (true for faint magnitudes, $K_p > 13$). We do not expect to find a solar twin when we horizontally move that far from the dashed line. (F. Bastien 2014, private communication). Our flicker diagram should be encompass solar dwarfs at different age-points and different activity levels. Two stars from this sample are confirmed to be quite similar to 18 Sco by Nogami *et al.* (2014), based on HDS@SUBARU observations.

6. ROTATION–AGE RELATIONSHIP FOR SOLAR ANALOGS

The rotation rates of these stars permit a deeper understanding of this sample. In Figure 1 we show the evolution of the averaged rotation period $\langle P_{\rm rot} \rangle$ for dwarfs and subgiants. The $\langle P_{\rm rot} \rangle$ increases ($21d \rightarrow 26d \rightarrow 32d \rightarrow 49d$) as stars evolve up the giant branch. This figure shows

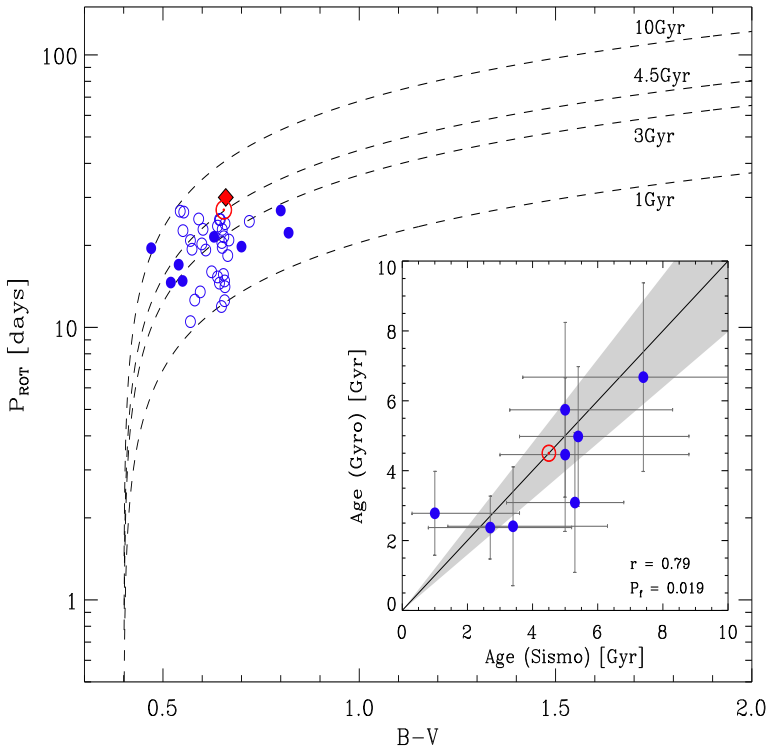

Figure 3. Color—period diagram for the seismic sample for which there are *Tycho* photometry (Høg *et al.* 2000) and solar analogs. The inside panel shows a comparison between gyro and seismic–ages for the seismic sample stars with a shaded region showing a ± 20% error.

the broad trend, constrained by sample size, of the $P_{\rm rot}$ of the subgiants. However, our real interest, as far as solar analogs and twins are concerned, is in understanding the dwarfs. The $\langle P_{\rm rot}\rangle$ for dwarfs is slightly lower than the solar rotation period. The $P_{\rm rot}$ that we have measured from the *Kepler* light curves, together with some solar proxies, permit an independent (from classical isochrone or seismic ages) age derivation for the dwarfs using gyrochronology (Kraft 1967; Skumanich 1972; Barnes 2007). The basic idea displayed in Figure 3 is that the, $P_{\rm rot}$ of cool stars are a function of the star's age and mass, allowing the age to be determined if the other two variables are known. In this work, we bypass the uncertainties in the color determination by working directly with $T_{\rm eff}$, converting it to the global convective turnover times τ using the Table 1 in Barnes & Kim (2010b), and then calculating the age using Equation (32) provided in Barnes (2010). For P_0, we used a value of 1.1days, as suggested in Barnes (2010). Remember that, in principle, gyrochronology only provides good results for main–sequence stars with masses less than about 1.2 $M_{\odot}$. These gyro-ages for dwarfs are listed in Table 1, along with the uncertainties originating in the $T_{\rm eff}$ and $P_{\rm rot}$ uncertainties. The inset in Figure 3 displays a comparison between the seismic- and gyro–ages on a star-by-star basis. The two ages are in agreement within the errors, with a correlation coefficient of $r = 0.79$ with a significance level of $P_f = 0.019$. The dwarf ages range from under 1 Gyr to 10 Gyr, with a median of roughly 3.9 Gyr, implying that this sample indeed consists of stars that are comparable in age to the Sun. For 35 dwarf stars from the KIC, we computed isochrone ages from the model described in Section. 3 (Figure 1) and gyro-ages (Barnes 2007; Meibom *et al.* 2011). Figure 4 is consistent with the theoretical predictions of van Saders & Pinsonneault (2013). As we expected, the isochrone ages are subject to huge systematic errors, reflected in the scattered open circles in Figure 4, coupled with the fact that stellar rotation has a strong dependence on mass.

7. CONCLUSIONS

We report rotation periods for 30 subgiants and 43 dwarfs, where 34 are main-sequence stars with $0.90 \leq M/M_{\odot} \leq 1.10$. For dwarfs, we determine individual masses and ages. This resulted in the identification of a new sample of at least 22 new solar twin candidates. Eight of these dwarfs stars (seismic sample) have asteroseismic ages determined by Chaplin *et al.* (2014) and allow a direct comparison between gyro and seismic-ages. The comparison shows reasonable agreement, mostly within 20% and with a correlation coefficient $r = 0.79$. $P_{\rm rot}$ for these samples, permit a general elucidation of how the $\langle P_{\rm rot}\rangle$ increase as solar analogs evolve during the main-sequence and subgiant phases. The sample of dwarfs contains stars with $P_{\rm rot}$ as slow as 27 days, however, the $P_{\rm rot}$ histogram distribution for our 43 main-sequence stars indicates a peak in 19 days, making these stars slightly younger than the Sun. This agree with Soderblom (1985), who reported that the Sun is within 1σ standard deviation of stars of its mass and age. The flicker of these stars is also measured and provides a new additional parameter in the search for solar twins based on its activity. This can be quite useful in future missions such as PLATO (Rauer *et al.* 2013).

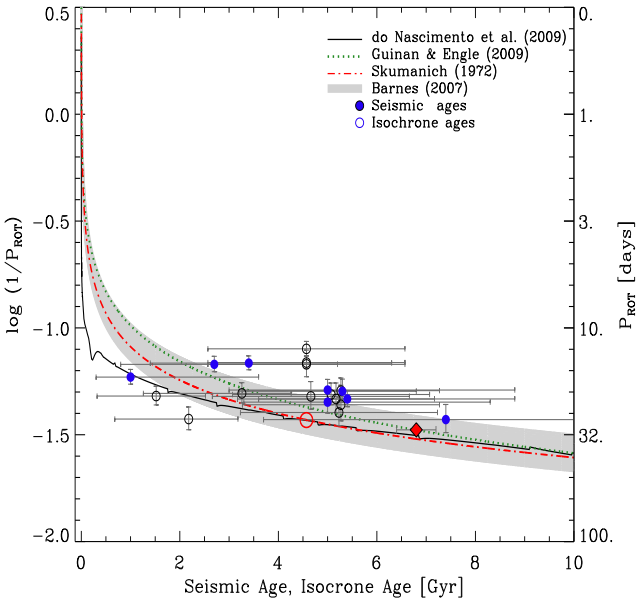

Figure 4. Angular velocity of dwarfs with 1.0 $M_{\odot}$ as a function of stellar age. Filled circles represent the seismic sample dwarfs. Open circles represent solar twin candidates. The shaded region represents the gyro relations (Barnes 2007) with $(B-V) = 0.642$ for the Sun, with $0.95 \leq M/M_{\odot} \leq 1.10$. Diamonds indicate 16 Cyg A and B.

The authors wish to thank the *Kepler* team. J.D.N. acknowledges CNPq Universal-B 485880/2012–1 and PDE 237139/2012. R.A.G. acknowledges the European Community Seventh Framework Program (FP7/2007-2013) no. 269194 (IRSES/ASK), and a CNES/*CoRoT* grant. S.M. was supported by NASA grant NNX12AE17G. J.D.N. is grateful to B. Chaplin and S. Saar for discussions and suggestions. This is a part of *Kepler* KASC Workpackage PE11.5 led by J.D.N. This paper is in memoriam of Giusa Cayrel de Strobel. Astronomer and pioneer in research on solar twins.

REFERENCES

Baglin, A., P., et al. 2006, in ESA Pub., Vol. 1306, 33
Barnes, S. A. 2007, ApJ, 669, 1167
Barnes, S. A. 2010, ApJ, 722, 222
Barnes, S. A., & Kim, Y.-C. 2010b, ApJ, 721, 675
Basri, G., Walkowicz, L. M., Batalha, N., et al. 2011, AJ, 141, 20
Bastien, F. A., Stassun, K. G., et al. 2013, Nature, 500, 427
Bazot, M., Ireland, M. J., Huber, D., et al. 2011, A&A, 526, L4
Borucki, W. J., Koch, D., Basri, G., et al. 2010, Science, 327, 977
Brown, T. M., Latham, D. W., et al. 2011, AJ, 142, 112
Cayrel de Strobel, G. 1996, A&A Rev., 7, 243
Chaplin, W. J., Basu, S., Huber, D., et al. 2014, ApJS, 210, 1
Christiansen, J. L., Van Cleve, J. E., Jenkins, J. M., et al. 2013, *Kepler* Data Characteristics Handbook, KSCI-19040-004
Cranmer, S. R., Bastien, F. A., et al. 2014, ApJ, 781, 124
do Nascimento, J. -D., Jr., Castro, M., et al. 2009, A&A, 501, 687
do Nascimento, J. -D., Jr., Takeda, Y., et al. 2013, ApJ, 771, 31
Dorren, J. D., & Guinan, E. F. 1994, ApJ, 428, 805
García, R. A., Hekker, S., Stello, D., et al. 2011, MNRAS, 414, 6
García, R. A., Ceillier, T., et al. 2014, arXiv1403.7155
Grevesse, N., & Noels, A. 1993, Origin and Evolution of the Elements, eds. N. Prantzos, E. Vangioni–Flam, and M. Cassé, Cambridge Univ. Press, p. 15
Guinan, E. F., & Engle, S. G. 2009, IAUS, 258, 395
Gustafsson, B. 2008, Physica Scripta Volume T, 130, 014036
Hardorp, J. 1978, A&A, 63, 383
Høg, E., Fabricius, C., Makarov, V. V., et al. 2000, A&A, 355, 27
Huber, D., Silva Aguirre, V., et al. 2014, ApJS, 211, 2
Hui-Bon-Hoa, A. 2008, Ap&SS, 316, 55
Jenkins, J. M., Caldwell, D. A., et al. 2010, ApJ, 197, 6
Kawaler, S. D. 1988, ApJ, 333, 236
Kraft, R. P. 1967, ApJ, 150, 551
Lund, M. N., Kjeldsen, H., et al. 2014, ApJ, 782, 2
Mathur, S., García, R. A., Régulo, C., et al. 2010, A&A, 511, 46
Mathur, S., Hekker, S., et al. 2011, ApJ, 741, 119
McQuillan, A., Mazeh, T., et al. S. 2013, ApJ, 775, 11
Meibom, S., Barnes, S. A., et al. 2011, ApJ, 733, L9
Meléndez, J., & Ramírez, I. 2007, ApJ, 669, L89
Metcalfe, T. S., Chaplin, W.J., et al. 2012, ApJ, 748, 10L
Monroe, T. R., Meléndez, J., et al. 2013, ApJ, 774L, 32
Nogami, D., Notsu, Y., et al. 2014, 2014arXiv1402.3772N
Noyes, R. W., Hartmann, L. W., et al. 1984, ApJ, 279, 763
Porto de Mello, G. F., & da Silva, L. 1997, ApJ, 482, L89
Ramírez, I., Michel, R., Sefako, R., et al. 2012, ApJ, 752, 5
Rauer, H., Catala, C., Aerts, C., et al. 2013, arXiv1310.0696
Richard, O., Vauclair, S., et al. 1996, A&A, 312, 1000
Scargle, J. D. 1982, ApJ, 263, 835
Silva Aguirre, V., Casagrande, L., et al. 2012, ApJ, 757, 99
Skumanich, A. 1972, ApJ, 171, 565
Soderblom, D. R. 1985, AJ, 90, 2103
Soderblom, D. R. 2010, ARA&A, 48, 581
Talon, S., Zahn, J.-P. 1997, A&A, 317, 749
van Saders, J., & Pinsonneault, M. 2013, ApJ, 776, 67
Wilson, O. C. 1963, ApJ, 138, 832

Table 1 Rotation of solar analogs and twin candidates revealed by *KEPLER*

N^{o} §	KIC	$V^{(\dagger)}$ (mag)	T_{eff} (K)	$\log g$ (dex)	$P_{rot}^{(\star)}$ $(days)$	S_Age, I_Age (Gyr)	$Gyro\_Age^{(\star)}$ (Gyr)	$F_{8hr}^{(\star)}$ (ppt)	$Mass^{(\star)}$ $(M_{\odot})$
1	2718678	11.493	6105^{+137}_{-177} $^{(\sharp)}$	$4.431^{+0.060}_{-0.286}$ $^{(\sharp)}$	$24.5^{+2.50}_{-2.50}$	$1.9^{+1.0}_{-1.5}$ $^{(\star)}$	$7.91^{+4.0}_{-4.0}$	$0.057^{+0.007}_{-0.007}$	$1.03^{+0.07}_{-0.08}$
2	3118654	13.235	5775^{+154}_{-157} $^{(\sharp)}$	$4.407^{+0.090}_{-0.260}$ $^{(\sharp)}$	$15.6^{+1.51}_{-1.51}$	$6.2^{+2.0}_{-2.0}$ $^{(\star)}$	$1.87^{+0.5}_{-0.5}$	$0.156^{+0.018}_{-0.018}$	$0.99^{+0.08}_{-0.07}$
3	4473226	15.707	5776^{+172}_{-169} $^{(\sharp)}$	$4.456^{+0.071}_{-0.269}$ $^{(\sharp)}$	$15.3^{+1.27}_{-1.27}$	$3.5^{+2.0}_{-2.0}$ $^{(\star)}$	$1.80^{+0.4}_{-0.4}$	$0.493^{+0.051}_{-26.910}$	$0.90^{+0.10}_{-0.10}$
4	5084157	11.649	6054^{+137}_{-137} $^{(\phi)}$	$4.202^{+0.018}_{-0.019}$ $^{(\phi)}$	$22.3^{+2.85}_{-2.85}$ $^{(\chi)}$	$5.0^{+3.3}_{-1.7}$ $^{(\phi)}$	$5.74^{+2.5}_{-2.5}$	$0.057^{+0.002}_{-0.002}$	$1.12^{+0.10}_{-0.08}$
5	5184732	8.165	5818^{+190}_{-190} $^{(\phi)}$	$4.257^{+0.012}_{-0.012}$ $^{(\phi)}$	$19.8^{+2.43}_{-2.43}$	$5.3^{+1.5}_{-2.1}$ $^{(\phi)}$	$3.09^{+1.1}_{-1.1}$	$0.033^{+0.001}_{-0.001}$	$0.99^{+0.10}_{-0.08}$

Note. — Table 1 is published in its entirety in the electronic edition of ApJL. A portion is shown here for guidance regarding its form and content.$^{(\star)}$ This paper; $^{(\dagger)}$ *Kepler* Input Catalogue; $^{(\phi)}$ Chaplin *et al.* (2014); $^{(\sharp)}$ Huber *et al.* (2014); $^{(\flat)}$ Metcalfe *et al.* (2012).; $^{(\chi)}$ half period detected; $^{(\psi)}$ twice period detected; $^{(\mu)}$ low modulation; $^{(\rho)}$ bad correction